



Original Paper

Evaluation and Assessment of Blast-Induced Ground Vibrations in an Underground Gold Mine: A Case Study

Jarryd Tribe,¹ Larissa Koroznikova,¹ Manoj Khandelwal^{1,2} and Jason Giri¹

Received 18 March 2021; accepted 28 August 2021

Published online: 21 September 2021

Ground vibrations induced during rock fragmentation by blasting remain a potential source of hazard for the stability of nearby structures. In this paper, to forecast the effect of blast-induced ground vibrations, dimensional analysis (DA) is proposed to predict peak particle velocity (PPV). In conventional predictor equations, the major and critical parameter for the estimation of PPV is square root scaled distance. The new formula based on DA was obtained considering various blast design parameters in order to improve the capability of PPV prediction. After obtaining the new DA equation for the prediction of PPV, 360 data sets were used to determine the unknown coefficients of the new equation as well as site constants of different conventional predictor equations. Then, ten additional randomly selected data sets were used to compare the capability of the new model with conventional predictor equations. The results were compared based on coefficient of determination (R^2) and mean absolute error (MAE) between measured and predicted values of PPV. The proposed formula with the greatest R^2 and the lowest MAE was the better option for predicting the PPV of induced vibrations for the measured field data.

KEY WORDS: Blast vibration, Underground mine, Dimensional analysis, Conventional predictors.

INTRODUCTION

Several mining companies encounter blast-induced ground vibration problems in the form of both social and environmental impacts on nearby residential areas. Blasting is an essential fragmentation and displacement process of rock to enable more efficient excavation in mining operations (Afeni & Osasan, 2009). Blast vibration levels need to be accurately monitored and reduced to a level that is suitable for both the local community and the mining company.

Blasting is a complex phenomenon that is controlled by a multitude of variables. The difficulty in predicting and controlling the vibration levels is influenced largely by the nature of rock at different geological conditions. Several methods are used to assess the influences of ground vibrations, but peak particle velocity (PPV) is the most preferred kinematic descriptor of ground motion (Saadat et al., 2014). The determination of PPV is therefore of particular importance to mining engineers when designing blasting parameters (Khandelwal, 2012). It was suggested that the distance between the blast location and the monitoring point, coupled with the maximum charge of explosives, are the two main factors that influence PPV primarily, where the level of effect can be influenced directly by the quantity of explosives used (Khandelwal & Singh, 2007).

¹School of Engineering, Information Technology and Physical Sciences, Federation University Australia, Ballarat, VIC 3350, Australia.

²To whom correspondence should be addressed; e-mail: m.khandelwal@federation.edu.au, mkhandelwal1@gmail.com

There are three factors that influence predominantly the degree of shaking, namely PPV, its frequency and its duration (Saadat et al., 2015). Mining operations near residential areas are bound by rules and regulations that prohibit excessive vibration levels (Chen et al., 2015). Altering blast timing sequences and parameters, such as size, depth, orientation, layout, location and number of holes, can potentially play a major role in controlling PPV levels. The geology of the surrounding rock also needs to be taken into account to strengthen conclusions made (Simangunsong & Wahyudi, 2015). However, these geological features constantly change due to the blast locations, meaning that a model suited to a general scenario lacks credibility. Studies undertaken on the predictive capabilities of various models are required for each new mine location. It is very challenging to predict the PPV levels precisely due to the uncertainty of various factors that affect vibration force.

Several benefits will arise if accurate predictions of PPV can be made. The effectiveness of blasting operations will increase as the safety factors set for predicted vibrations levels can be lowered. This can increase profit margins for mining companies by allowing engineers to optimize blasting parameters to achieve more effective and efficient outcomes, and at the same time reduce social and environmental impacts (Mohamed, 2009; Khandelwal, 2011; Khandelwal et al., 2011; Monjezi et al., 2013).

Several models can be used to predict vibration levels, and the accuracy of each model varies for different geological conditions. Many conventional predicting equations have been developed over the years based on explosive charge used per delay and distance between blast face to monitoring point, but in recent times improved models have been used to reduce the variance in the predicted results. One of the main reasons for this improvement is largely due to the increased number of parameters used to provide a more accurate description of the wave propagation effect. Many researchers (Monjezi et al., 2006; Khandelwal & Singh, 2006, 2007, 2009, 2013; Khandelwal, 2010, 2012; Khandelwal et al., 2010, 2017; Fisne et al., 2011; Álvarez-Vigil et al., 2012; Bakhshandeh et al., 2012; Mohamadnejad et al., 2012; Armaghani et al., 2015; Bakhtavar et al., 2017a, 2017b; Bakhtavar & Yousefi, 2019; Ding et al., 2020; Fang et al., 2020; Rezaeineshat et al., 2020; Zhang et al., 2020; Bayat et al., 2021; Bui et al., 2021; Fattahi et al., 2021; He et al., 2021; Qiu et al., 2021) have applied various artificial intelligence

techniques, such as artificial neural networks (ANNs) and support vector machines (SVMs), to study PPV. It was found that the maximum charge per delay and distance between the blast face to the monitoring point are important, but other parameters, such as stemming, hole depth, physical and mechanical properties of rock mass, burden and spacing, can also alter the intensity of ground vibration. It is very strenuous to obtain a PPV equation based on all the affected parameters using an ANN, despite its capability in function approximation and prediction of nonlinear relationships among various parameters.

Dehghani and Ataee-pour (2011) developed a PPV predictor equation using dimensional analysis (DA). It was proposed that empirical methods are not suitable due to the large number of important parameters that can affect vibration levels. They selected various input model parameters based on an artificial neural network (ANN) approach. The study established that the effectiveness of the DA model decreased when parameters have limited correlations with vibration levels. Therefore, choosing variables with high correlation effect is particularly important to the success of any model. It was found that when ANN was used to remove all unnecessary variables, the DA model produced much higher levels of correlation compared to using any of the conventional predictor equations. DA was applied successfully by Khandelwal and Saadat (2015) to approximate the effects of blast-induced ground vibrations. The Buckingham *Pi* theorem was employed to create dimensionless groups. Both linear and nonlinear regression analysis were used to relate these groups, but the nonlinear method was more accurate compared to the linear approach. They also compared the proposed model to other conventional models and found that the DA approach can be suitable for predicting PPV. A similar DA approach was undertaken by Cheng and Chau (2015), who established the approach is feasible. Their aim was to construct a new empirical formula for a standardized PPV, which is dimensionless. The used 500 blast vibration data measurements from the Anderson Road Quarry in Hong Kong to compare the accuracy of the results using conventional and new dimensionless formulas. The parameters considered were explosive energy, duration times and densities of rock. It was realized that the proposed approach obtained better PPV estimates with a correlation coefficient of 0.9509 as opposed to 0.7607 for the conventional methods. Bakhtavar et al.,

(2017a, 2017b) applied a hybrid DA fuzzy inference system to study and predict blast-induced flyrock in a copper mine based on 320 data sets and found that flyrock predictions by the system were in close agreement with real measurements. Sanchidrián and Ouchterlony (2017) developed a DA approach to study rock fragmentation in bench blasting. Their model could be used from 5 to 100 percentile sizes range with an expected error of < 25% at any percentile. Bakhtavar et al. (2015) applied a DA approach along with multivariate nonlinear regression analysis to study and predict rock fragmentation of Sungun surface mine. They developed a rock fragmentation equation by incorporating various independent dimensionless products derived from DA and compared their fragmentation prediction results with sieve analysis, image processing technique as well as the Kuz-Ram model. They found that their prediction outcome was closer to actual fragmentation results obtained from sieve analysis compared to the other models. Thus, DA has been utilized extensively in the past to analyze complex relationships among various physics-based quantities. The DA method identifies the base quantities of the different variables, where different procedures can be applied to combine certain variables into a form that has dimensionless units in order to facilitate the interpretation and extend the range of application of experimental data (Alhama & Madrid, 2007).

In the present study, a DA approach was exercised to study and assess PPV in an underground gold mine in Australia using various blast design parameters. The novelty of this research work is that both linear and nonlinear DA approaches have been applied to predict and assess blast vibrations in an underground gold mine. Then, a simple and easy-to-use blast vibration equation is proposed based on DA. A comparative analysis of the newly proposed equation and conventional empirical models was performed to obtain the prediction capability of each model.

DIMENSIONAL ANALYSIS

DA is an engineering problem solving method that examines complex relationships among a set of physical quantities (Sharp et al., 1992). The procedure involves manipulating the individual variables involved in the problem, whereby the relationships are simplified into an equation that involves a smaller number of dimensionless parameters. The

Buckingham *Pi* theorem is a method that is used when a large number of independent variables is present (Reddy & Reddy, 2014). This theorem is one of the many methods that can be used to develop dimensionless variables. In mathematical terms, the Buckingham *Pi* theorem states that if a number of measurable quantities (or variables) form a complete functional relationship shown in Eq. (1), then the solution has the form of Eq. (2) (Dehghani & Ataee-pour, 2011), thus:

$$\varphi(A, B, C, \dots) = 0 \quad (1)$$

$$f(\pi_1, \pi_2, \pi_3, \dots) = 0 \quad (2)$$

where the terms A , B and C are, in this study, the various variables that affect vibration levels. The π terms in Eq. (2) are the dimensionless groups that represent the products of the A , B and C terms. If there are enough fundamental units to describe the magnitude of the quantities considered, then Eq. (2) can represent a complete relationship.

Dimensional quantities employed in DA are represented by m and the variables associated with these quantities are denoted by n . Once the dimensional quantities have been established, they need to be transformed into a combination of either force, length or time. The number of π terms is equal to the difference between the number of measurable variables and fundamental units. Equation (3) is a mathematical representation of this definition, where “ r ” is the number of π dimensionless terms, thus:

$$r = n - m \quad (3)$$

Once the desired variables have been chosen, they are placed in matrix form where the fundamental quantities make up the rows and each variable forms the columns. The powers of the fundamental dimensions m corresponding to each variable n are used to construct the matrix (Eq. (3)).

Among the n variables, a number of so-called “repeating variables” are chosen. The number of repeating variables chosen is equivalent to the number of fundamental quantities m . These repeating variables will appear in all the π terms and must be chosen based on the following two restricting rules. First, all repeating variables must have dimensions; they cannot be dimensionless. Second, the overall dimensions of each repeating variable must have different combinations of dimensions compared to all other variables used in

the procedure. Once the repeating variables have been selected, the determinant of their fundamental dimensions can be calculated. If the determinant of the square matrix is not equal to zero, then the rows of the matrix are linearly independent. If the determinant is found to be zero, then a different set of repeating variables needs to be considered.

Once all the prerequisite information has been identified, the dimensionless π variables can be calculated. By selecting one of the non-repeating variables (D) and assuming there are three repeating variables (A, B, C), the first π dimensionless group can be calculated as:

$$\pi_1 = [A]^{a_1} \cdot [B]^{b_1} \cdot [C]^{c_1} \cdot [D] \tag{4}$$

The second dimensionless group can be calculated by once again multiplying the three repeating variables by the next non-repeating variable (E), thus:

$$\pi_2 = [A]^{a_2} \cdot [B]^{b_2} \cdot [C]^{c_2} \cdot [E] \tag{5}$$

Note that the subscript for the a, b, c constants relates to the subscript for the π groups. The procedure for Eqs. (4)–(5) is continued for all the remaining variables. For the π variables to be dimensionless, the summation of the powers represented by “ a, b, c ” in the equations needs to be eliminated. By doing this, the “ a, b, c ” constant will multiply each variable in the group in such a way that the π group will be dimensionless.

Once each π group has been made dimensionless, they need to be manipulated to form an equation. The method chosen to relate these variables is multiple regression analysis. A typical linear regression equation has the form:

$$y = k + x_1 \cdot (\pi_1) + x_2 \cdot (\pi_2) + \dots + x_r \cdot (\pi_r) \tag{6}$$

where the r subscript is the number of dimensionless groups determined from Eq. (3) and the x variables are the site constants. Nonlinear regression analysis can also be used, thus:

$$\ln(y) = k + x_1 \cdot \ln(\pi_1) + x_2 \cdot \ln(\pi_2) + \dots + x_r \cdot \ln(\pi_r) \tag{7}$$

Linear Regression Analysis

To determine the site constants, a regression analysis toolpack of Microsoft Excel 2016 was applied. The recorded data were entered into Excel, as

Table 1. Recorded data used to determine the site constants for the DA equation

No	A	B	C	...
1	A1	B1	C1	...
2	A2	B2	C2	...
3	A3	B3	C3	...
⋮	⋮	⋮	⋮	⋮

Table 2. Dimensionless variables added to the Excel sheet

No	A	B	C	...	π_1	...	π_r
1	A1	B1	C1	...	= A1 × B1 × C1	...	= π_{r_1}
2	A2	B2	C2	...	= A2 × B2 × C2	...	= π_{r_2}
3	A3	B3	C3	...	= A3 × B3 × C3	...	= π_{r_3}
⋮	⋮	⋮	⋮	...	⋮	...	⋮

per the format shown in Table 1. The columns are all the variables considered and the rows are the iterations of each test.

For linear regression analysis, a new set of columns needs to be created to the right of the measured variables. Each new column is a dimensionless π group. For example, if the first π group was found to have a dimensionless combination of $A \times B \times C$, then the new column would have this combination as a result. The formula in Excel used for this example is shown in Table 2. This process is completed for all dimensionless groups.

Once Table 2 is completed, the data analysis tool can be used as it is able to compute a regression analysis on the dimensionless groups. To run this regression analysis, two sets of variables are required. The Y input range comprises the dependent variables and the X input range comprises all the other variables that are independent of the Y values.

The problem with Buckingham Pi theorem is that the dependent variable is typically one of the variables within one of the dimensionless groups. If it is assumed that variable B is the dependent variable, then it means that the π_1 column needs to be adjusted to make the B value by itself. This means that, before the regression can be run, the independent dimensionless groups must be modified. If $\pi_1 = A \times B \times C$, where B is the dependent variable, then the operation to get B by itself is:

$$f(\pi_1 \div (A \times C), \pi_2 \div (A \times C), \dots, \pi_r \div (A \times C)) = 0 \tag{8}$$

Table 3. Modified Excel spreadsheet to allow linear regression analysis to be run

No	A	B	C	...	$\pi_1 \div (A \times C)$...	$\pi_r \div (A \times C)$	y
1	A1	B1	C1	...	$= \frac{A1 \times B1 \times C1}{(A1 \times C1)}$...	$= \pi_{r1} \div (A1 \times C1)$	y1
2	A2	B2	C2	...	$= \frac{A2 \times B2 \times C2}{(A2 \times C2)}$...	$= \pi_{r2} \div (A2 \times C2)$	y2
3	A3	B3	C3	...	$= \frac{A3 \times B3 \times C3}{(A3 \times C3)}$...	$= \pi_{r3} \div (A3 \times C3)$	y3
⋮	⋮	⋮	⋮	...	⋮	...	⋮	⋮

This means that the same operation performed on π_1 to get B by itself must also be applied to the other dimensionless groups. The Excel spreadsheet can be updated using Eq. (8) (Table 3).

Running the regression analysis produces the same number of coefficients as the number of modified independent variables, plus an additional intercept coefficient k . Using the above example, Eq. (6) becomes:

$$y = k + x_2 \cdot \left[\frac{\pi_2}{(A \times C)} \right] + x_3 \cdot \left[\frac{\pi_3}{(A \times C)} \right] + \dots + x_r \cdot \left[\frac{\pi_r}{(A \times C)} \right] \tag{9}$$

where y is the predicted variable, k is the intercept coefficient generated by Excel and the x coefficients are the site constants that relate to each independent variable selected when running the regression. The terms in brackets in Eq. (9) are no longer the original dimensionless groups. They are now the modified dimensionless groups. The site constants k and x are related to the modified groups, not the original groups. This is true for the predicted variable as well. Y is not the same as π_1 , because replacing π_1 means that all the site constants are affected as well.

Nonlinear Regression Analysis

Nonlinear regression analysis follows the same process as the linear one, but the former takes the natural logarithm of each dimensionless group, which alters Eq. (2) into:

$$f(\ln(\pi_1), \ln(\pi_2), \dots, \ln(\pi_r)) = 0 \tag{10}$$

Using Eq. (10), Table 2 can be modified into Table 4.

Again, assuming $\pi_1 = A \times B \times C$ and B is the dependent variable, Eq. (10) is modified to get $\ln(B)$ by itself as:

Table 4. Natural logarithms of the dimensionless groups

No	A	B	C	...	$Ln(\pi_1)$...	$\ln(\pi_r)$
1	A1	B1	C1	...	$= \ln(A1 \times B1 \times C1)$...	$= \ln(\pi_{r1})$
2	A2	B2	C2	...	$= \ln(A2 \times B2 \times C2)$...	$= \ln(\pi_{r2})$
3	A3	B3	C3	...	$= \ln(A3 \times B3 \times C3)$...	$= \ln(\pi_{r3})$
⋮	⋮	⋮	⋮	...	⋮	...	⋮

$$\ln(\pi_1) = \ln(A \times B \times C)$$

$$\ln(A \times B \times C) = \ln(A) + \ln(B) + \ln(C)$$

$$\ln(B) = \ln(\pi_1) - \ln(A) - \ln(C)$$

$$\therefore f([\ln(\pi_1) - \ln(A) - \ln(C)], [\ln(\pi_2) - \ln(A) - \ln(C)], \dots, [\ln(\pi_r) - \ln(A) - \ln(C)]) = 0$$

Thus, the appropriate columns in Table 4 are modified as shown in Table 5.

The predicted variable y can be calculated using Eq. (7), thus:

$$\ln(y) = k + x_2 \cdot [\ln(\pi_2) - \ln(A) - \ln(C)] + \dots + x_r \cdot [\ln(\pi_r) - \ln(A) - \ln(C)]$$

To get the predicted variable by itself, the exponential of both sides can be taken as:

$$y = \exp(k + x_2 \cdot [\ln(\pi_2) - \ln(A) - \ln(C)] + \dots + x_r \cdot [\ln(\pi_r) - \ln(A) - \ln(C)])$$

where the y value is the predicted variable, k is the intercept coefficient generated by Excel, and the x coefficients are the site constants that relate to each independent variable selected when running the regression.

Table 5. Modified dimensionless groups to allow nonlinear regression analysis to be performed

No	A	B	C	...	$\ln(\pi_1) - \ln(A) - \ln(C)$...	$\ln(\pi_r) - \ln(A) - \ln(C)$
1	A1	B1	C1	...	$\ln(A1 \times B1 \times C1) - \ln(A1) - \ln(C1)$...	$\ln(\pi_{r_1}) - \ln(A1) - \ln(C1)$
2	A2	B2	C2	...	$\ln(A2 \times B2 \times C2) - \ln(A2) - \ln(C2)$...	$\ln(\pi_{r_2}) - \ln(A2) - \ln(C2)$
3	A3	B3	C3	...	$\ln(A3 \times B3 \times C3) - \ln(A3) - \ln(C3)$...	$\ln(\pi_{r_3}) - \ln(A3) - \ln(C3)$
⋮	⋮	⋮	⋮	...	⋮	...	⋮

Conventional Predictors

Conventional predictor equations are all in the form of a basic power function, thus:

$$y = a \cdot (x)^b \tag{11}$$

where the terms *a* and *b* are site constants and *x* represents various scaled distance combinations with respect to total explosives used per delay. Table 6 highlights some of the common conventional predictor equations proposed by various researchers.

FIELD STUDY

The study was conducted at one of the underground gold mines in Australia. The mineralization transpires within the lower Ordovician mudstones, sandstones and siltstones, which have been metamorphosed and tightly folded around a north-dipping axis. Of all the known western segments of the anticlines, the dip is roughly 70°W; the dip in the eastern sectors range from 85°W to 85°E, and the folded axial planes dip approximately 80°W. The regional strike of the bedding is in a northerly direction. The mineable quartz veins occurring lodes and stockworks typically located within folded sections. The lodes and stockworks exist in west-dipping fault zones. The mineralization is characterized by notable coarse gold contained in the quartz veins. In some sections, a high nugget effect is found with grades reaching 50 g/t or higher over a few meters.

Due to the proximity of the mine to the residential area, the vibration levels and noise produced from the mine operations have strict licensing conditions. At the higher end of the scale are the blast vibration levels, where current restrictions prevent vibration levels from exceeding 10 mm/s at any time and no more than 5% of blasts are permitted to exceed 5 mm/s over a 12-month period. In addition, the maximum blast vibration levels between the hours of 10:00 pm and 7:00 am are 3 mm/s.

At the mine, the production blasting method is an open stoping technique that follows the veins of the gold ore. Once the ore has been mined out the open stope is backfilled, allowing for the next section of the vein to be blasted and mined out. The hole lengths generally range from 10 to 25 m and depend on local ground conditions and orientations of the ore lodes. The diameters of the blast holes are 76 mm. Production blast holes use programmable electronic detonators inserted into a cast primer. Most of the hole is then filled with either ANFO or an impact 50/50 blend depending on the required output. Due to the large sections of rock requiring fragmentation, production blasts typically produce much higher PPV than ordinary development blasts.

Development blast holes are typically 3.7 m in length with 45 mm diameter. These blast holes use non-electronic development detonators connected to an electric detonating cord, which sets off each hole based on the preset delay sequence. Due to the low quantity of explosives used, development blasting practices rarely raise cause for concern and thus are not analyzed for predictions of the PPV.

At the mine, approximately two development blasts per shift are completed, whereas the number of production blasts is approximately two per week. In various locations around the neighboring houses, monitoring instruments are used to measure blast-induced ground vibrations. These instruments are highly sensitive and can on occasion record vibration levels that are not related to blasting activities such as a vehicle driving past. For each production blast, a plethora of variables are recorded, and some of the important variables are listed in Table 7. In conjunction with these variables, the locations within the mine and the monitoring site are also recorded. The blasting parameters for production are highly specialized and are designed to allow for appropriate fragmentation of the surrounding rock. This means that there is no set design for a production blast. These designs can incorporate the number of holes, the diameter of these holes and their lengths, as well as the burden and spacing dimensions for these holes.

Table 6. Conventional predictor equations used for this study

Name	Equation
United States Bureau of mines (Duvall et al., 1962)	$PPV = K \left(\frac{D}{\sqrt{MIC}} \right)^{-B}$
Langefors–Kihlstrm (1963)	$PPV = K \left(\sqrt{\frac{MIC}{D^3}} \right)^B$
Ambraseys–Hendron (1968)	$PPV = K \left(\frac{D}{MIC^{\frac{1}{3}}} \right)^{-B}$
Bureau of Indian Standards (1973)	$PPV = K \left(\frac{MIC}{D^{\frac{1}{3}}} \right)^B$

MIC is maximum instantaneous charge per delay. *D* is distance between blast face to monitoring point. *K* and *B* are site constants, which can be determined by multiple regression

Table 7. Variables used to perform DA

Variable symbol	Variable	Unit	Dimension
PPV	Peak particle velocity	mm/s	$L \cdot T^{-1}$
θ	Number of holes	–	–
δ	Number of detonators	–	–
PF	Powder factor	kg/m ³	$F \cdot T^2 \cdot L^{-4}$
ch	Total ANFO used	kg	$F \cdot T^2 \cdot L^{-1}$
I	Impact 50/50	kg	$F \cdot T^2 \cdot L^{-1}$
De	Duration	s	T
MIC	Maximum instantaneous charge	kg	$F \cdot T^2 \cdot L^{-1}$
<i>D</i>	Distance to surface	m	L
R	Amount of rock blasted	kg	$F \cdot T^2 \cdot L^{-1}$

F force. *L* length. *T* time

The geological characteristics of the surrounding rock between the blast location and the monitoring site are extremely difficult to analyze. What can be examined and approximately measured is the powder factor, which is the amount of force required to adequately fracture the rock. The total tonnage of rock that needs to be fragmented can also be recorded.

The properties associated with the explosives can be evaluated, where the total amount of explosives can play an important role in affecting the peak vibration levels. If all the explosive content used was detonated at the same time, then the peak vibration level can be large. For this reason, there is a delay between sets of holes to prevent excessive vibration levels. The maximum instantaneous charge is recorded, which is the highest charge that can detonate at any given time. The explosives used are both ANFO and impact 50/50, which is an explosive mixture that contains some inert material. The 50/50 impact explosive has a lower explosive force than ANFO; the latter is employed if a more controlled fragmentation is required, which is generally within

the perimeters of the blast pattern. This ultimately reduces unnecessary fragmentation.

For the present study, 419 blast vibration data sets were acquired from December 31, 2014, to June 5, 2017, of which 360 data sets were examined to determine the site constants for the various models analyzed. The DA model was specifically designed for the mine; therefore, the variables chosen to develop the equation were based on the data that were previously been recorded (Table 7). To validate the accuracy of the DA model, another ten sets of data acquired from June 6, 2017, to August 29, 2017, were used to predict PPV. These new sets of data were also examined for the most effective conventional predictor equations, whereby the results of the two models were compared to one another.

ERROR ANALYSIS FOR COMPARING PREDICTOR MODELS

There are many error indices that can be applied to analyze the effectiveness of a prediction equation. As mentioned by Cheng et al. (2014), the

coefficient of determination (R^2) is an error analysis tool for judging how effective a regression line predicts the actual results. It aims to show the correlation of predicted value, s against actual measured values. The value of R^2 typically ranges between 0 and 1, where 1 indicates a perfect relationship and 0 no correlation. To calculate R^2 , the first step is to determine the correlation coefficient (r):

$$r = \frac{n \cdot \sum(x \cdot y) - \sum(x) \cdot \sum(y)}{\sqrt{[n \sum(x^2) - (\sum x)^2] \cdot [n \sum(y^2) - (\sum y)^2]}} \tag{12}$$

where n is the number of input/output variables, x represent predicted values and y represent actual measured values. Then, R^2 is computed as:

$$R^2 = \left(\frac{n \cdot \sum(x \cdot y) - \sum(x) \cdot \sum(y)}{\sqrt{[n \sum(x^2) - (\sum x)^2] \cdot [n \sum(y^2) - (\sum y)^2]}} \right)^2 \tag{13}$$

Expressing R^2 as a percentage shows what percentage of data points fall on the regression line. This value is an indicator of the likelihood a predicted value will fall on the regression line. However, the R^2 does not necessarily determine causality, even if the relationship is high. For this reason, another error analysis measurements can be applied. The mean absolute error (MAE) and root mean squared error (RMSE) can both be used in conjunction with the R^2 to provide a more accurate interpretation of the relationship between the predicted and actual variables. MAE and RMSE are calculated, respectively, as:

$$MAE = \frac{1}{n} \sum |y_j - \hat{y}_j| \tag{14}$$

$$RMSE = \sqrt{\frac{1}{n} \sum (y_j - \hat{y}_j)^2} \tag{15}$$

where n is the number of data points analyzed, y_j represents actual values and \hat{y}_j represents predicted values. The MAE and RMSE are two of the most commonly considered accuracy measures for continuous variables. The MAE indicates the average magnitude of errors between the predictions made and the actual results. The RMSE also measures the average magnitude of the error. However, but the

benefit of RMSE is that it squares the errors before they are averaged, which allows for the RMSE to assign a high weighting to large errors. This is highly desirable for this study as large errors need to be negated as much as possible. Because the MAE and RMSE are both negatively orientated, the lower their values, the better. In other words, if RMSE or MAE is zero, it means a perfect relationship.

RESULTS

Dimensional Analysis

The choice of variables used to develop the dimensionless groups was based on variables the gold mine had previously measured. These variables, with their common dimensions as well as their basic fundamental units, are shown in Table 7. Using Eq. (1), the functional relationships of these variables must therefore satisfy the following relationship:

$$\varphi(PPV, \theta, \delta, PF, ch, I, De, MIC, D, R) = 0$$

The matrix of these variables is presented in Table 8.

From the matrix in Table 8, there are three basic fundamental units, namely force, length and time. From Eq. (3), the total number of dimensionless π groups can be calculated as:

$$r = n - m$$

$$\therefore r = 10 - 3 = 7$$

where n is number of variables and m is number of basic fundamental units. Therefore, Eq. (2) is modified as:

$$f(\pi_1, \pi_2, \pi_3, \pi_4, \pi_5, \pi_6, \pi_7) = 0 \tag{16}$$

Only three of the variables in Table 8 satisfy the rules for choosing the repeating variables that will appear in each dimensionless group. These variables

Table 8. Matrix of fundamental dimensions of the chosen variables for DA

	PPV	θ	δ	PF	ch	I	De	MIC	D	R
F	0	0	0	1	1	1	0	1	0	1
L	1	0	0	-4	-1	-1	0	-1	1	-1
T	-1	0	0	2	2	2	1	2	0	2

are powder factor (PF), distance (D) and duration (De). The determinant of the matrix for these variables was found to be 1, thus:

$$\det \begin{vmatrix} 1 & 0 & 0 \\ -4 & 1 & 0 \\ 2 & 0 & 1 \end{vmatrix} = 1$$

Therefore, the rows of the matrix are linearly independent. Developing the dimensionless groups was thus undertaken as displayed in Table 9:

From Table 9, the dimensions for $\pi_2, \pi_3, \pi_4, \pi_5$ are all equal. This means that all the power constants a, b and c will be the same. π_6 and π_7 are dimensionless; therefore, the number of dimensionless groups is equal to the number of variables.

The power constants for π_1 is calculated as follows:

For force (F): $a_1 = 0$.

For time (T): $2 \cdot a_1 + c_1 - 1 = 0$.

For length (L): $-4 \cdot a_1 + b_1 + 1 = 0$.

By solving these system of equations, the power constants were found to be:

$$a_1 = 0, b_1 = -1, c_1 = 1.$$

Substituting these constant into the equation yields:

$$\pi_1 = [\text{PF}]^0 \cdot [D]^{-1} \cdot [\text{De}]^1 \cdot [\text{PPV}]$$

$$\therefore \pi_1 = \text{PPV} \cdot \frac{\text{De}}{D}$$

The power constants for π_2 is calculated as follows:

For force (F): $a_2 + 1 = 0$.

For time (T): $2 \cdot a_2 + c_2 + 2 = 0$.

For length (L): $-4 \cdot a_2 + b_2 - 1 = 0$.

By solving these system of equations, the power constants were found to be:

$$a_2 = -1, b_2 = -3, c_2 = 0.$$

Substituting these constants back into the equation yields:

$$\pi_2 = [\text{PF}]^{-1} \cdot [D]^{-3} \cdot [\text{De}]^0 \cdot [\text{MIC}]$$

$$\therefore \pi_2 = \frac{\text{MIC}}{\text{PF} \cdot D^3}$$

Therefore, the dimensionless groups were:

$$\begin{aligned} \pi_1 &= \text{PPV} \cdot \frac{\text{De}}{D} \\ \pi_2 &= \frac{\text{MIC}}{\text{PF} \cdot D^3} \\ \pi_3 &= \frac{R}{\text{PF} \cdot D^3} \\ \pi_4 &= \frac{\text{ch}}{\text{PF} \cdot D^3} \\ \pi_5 &= \frac{I}{\text{PF} \cdot D^3} \\ \pi_6 &= \theta \\ \pi_7 &= \delta \end{aligned}$$

From Eq. (6), the linear regression equation used to relate the dimensionless groups was:

$$\begin{aligned} \text{PPV} \cdot \frac{\text{De}}{D} &= k + \left(x_2 \cdot \frac{\text{MIC}}{\text{PF} \cdot D^3} \right) + \left(x_3 \cdot \frac{R}{\text{PF} \cdot D^3} \right) \\ &+ \left(x_4 \cdot \frac{\text{ch}}{\text{PF} \cdot D^3} \right) + \left(x_5 \cdot \frac{I}{\text{PF} \cdot D^3} \right) \\ &+ (x_6 \cdot \theta) + (x_7 \cdot \delta) \end{aligned} \tag{17}$$

Equation (17) is the linear DA equation.

From Eq. (7), the nonlinear regression equation used to relate the dimensionless groups was:

$$\begin{aligned} \ln \left(\text{PPV} \cdot \frac{\text{De}}{D} \right) &= k + x_2 \cdot \ln \left[\frac{\text{MIC}}{\text{PF} \cdot D^3} \right] + x_3 \cdot \ln \left[\frac{R}{\text{PF} \cdot D^3} \right] \\ &+ x_4 \cdot \ln \left[\frac{\text{ch}}{\text{PF} \cdot D^3} \right] \\ &+ x_5 \cdot \ln \left[\frac{I}{\text{PF} \cdot D^3} \right] + x_6 \cdot \ln[\theta] + x_7 \cdot \ln[\delta] \end{aligned} \tag{18}$$

Equation 18 is the nonlinear DA equation.

Equations (17) and (18) were modified to Eqs. (19) and (20), respectively, for PPV determination; thus:

$$\begin{aligned} \text{PPV} &= k - x_2 \cdot \left[\frac{\text{MIC}}{\text{PF} \cdot D^2 \cdot \text{De}} \right] - x_3 \cdot \left[\frac{R}{\text{PF} \cdot D^2 \cdot \text{De}} \right] \\ &+ x_4 \cdot \left[\frac{\text{ch}}{\text{PF} \cdot D^2 \cdot \text{De}} \right] + x_5 \cdot \left[\frac{I}{\text{PF} \cdot D^2 \cdot \text{De}} \right] - x_6 \cdot \left[\frac{\theta \cdot D}{\text{De}} \right] \\ &+ x_7 \cdot \left[\frac{\delta \cdot D}{\text{De}} \right] \end{aligned} \tag{19}$$

Table 9. Dimensionless groups with their respective dimensional quantities

Equation	Equation dimensions
$\pi_1 = [PF]^{a_1} \cdot [D]^{b_1} \cdot [De]^{c_1} \cdot [PPV]$	$\pi_1 = [F \cdot T^2 \cdot L^{-4}]^{a_1} \cdot [L]^{b_1} \cdot [T]^{c_1} \cdot [L \cdot T^{-1}]$
$\pi_2 = [PF]^{a_2} \cdot [D]^{b_2} \cdot [De]^{c_2} \cdot [MIC]$	$\pi_2 = [F \cdot T^2 \cdot L^{-4}]^{a_2} \cdot [L]^{b_2} \cdot [T]^{c_2} \cdot [F \cdot T^2 \cdot L^{-1}]$
$\pi_3 = [PF]^{a_3} \cdot [D]^{b_3} \cdot [De]^{c_3} \cdot [R]$	$\pi_3 = [F \cdot T^2 \cdot L^{-4}]^{a_3} \cdot [L]^{b_3} \cdot [T]^{c_3} \cdot [F \cdot T^2 \cdot L^{-1}]$
$\pi_4 = [PF]^{a_4} \cdot [D]^{b_4} \cdot [De]^{c_4} \cdot [ch]$	$\pi_4 = [F \cdot T^2 \cdot L^{-4}]^{a_4} \cdot [L]^{b_4} \cdot [T]^{c_4} \cdot [F \cdot T^2 \cdot L^{-1}]$
$\pi_5 = [PF]^{a_5} \cdot [D]^{b_5} \cdot [De]^{c_5} \cdot [I]$	$\pi_5 = [F \cdot T^2 \cdot L^{-4}]^{a_5} \cdot [L]^{b_5} \cdot [T]^{c_5} \cdot [F \cdot T^2 \cdot L^{-1}]$
$\pi_6 = [PF]^{a_6} \cdot [D]^{b_6} \cdot [De]^{c_6} \cdot [\theta]$	π_6
$\pi_7 = [PF]^{a_7} \cdot [D]^{b_7} \cdot [De]^{c_7} \cdot [\delta]$	π_7

Table 10. Site constants for the linear and nonlinear equations when all the data sets are considered

Constants	Linear	Nonlinear
k	1.016236426	2.333314519
x_2	- 1158.210237	- 0.176676485
x_3	- 67.63676108	0.003085455
x_4	455.358002	0.470737454
x_5	401.5024263	0.00682024
x_6	- 6.99488E-05	- 0.591729356
x_7	5.95367E-05	0.532142557

$$\begin{aligned} \ln(PPV) = & 2.33 - 0.18 \cdot \ln\left(\frac{MIC}{PF \cdot D^2 \cdot De}\right) + 0.003 \cdot \ln\left(\frac{R}{PF \cdot D^2 \cdot De}\right) \\ & + 0.47 \cdot \ln\left(\frac{ch}{PF \cdot D^2 \cdot De}\right) \\ & + 0.007 \cdot \ln\left(\frac{I}{PF \cdot D^2 \cdot De}\right) - 0.59 \cdot \ln\left(\frac{\theta \cdot D}{De}\right) \\ & + 0.53 \cdot \ln\left(\frac{\delta \cdot D}{De}\right) \end{aligned} \tag{22}$$

The predicted values PPV, by using Eqs. (21) and (22), were then compared to the actual measured variables (Figs. 1, 2).

The R^2 for the linear DA regression was 0.2542, whereas for the nonlinear DA regression it was 0.2915. The linear DA regression showed higher MAE and RMSE compared to non-linear DA regression. The errors associated with the linear and nonlinear predictions are reported in Table 11.

DA—Segregation of Site Constants for Comparable Conditions

The gold mine has four different sections within the mine. It also has nine different monitoring locations. Different combinations of monitoring locations with different mine sections were observed in the data. Therefore, the data were segregated to compare constant characteristics relating to distance between the blast location and the monitoring site. This generated a set of site constants for each comparison, thus, creating a variety of predictor equations. Comparisons of the predicted PPV results against the actual PPV results using these site constants are shown in Figures 3 and 4. From these figures, it can be said that the nonlinear DA regression showed higher R^2 compared to the linear DA regression. The MAE and RMSE were also lower for the nonlinear DA regression compared to

Linear and Nonlinear Regression Analyses Considering All Blasting Data sets

Multiple regression analysis in Microsoft Excel 2016 was used to develop the site constants for Eqs. (19) and (20) and is given in Table 10.

Therefore, the DA equations using the site constants generated in Excel (Table 10) are:

$$\begin{aligned} PPV = & 1.02 - 1158.2 \cdot \left[\frac{MIC}{PF \cdot D^2 \cdot De}\right] - 67.64 \cdot \left[\frac{R}{PF \cdot D^2 \cdot De}\right] \\ & + 455.36 \cdot \left[\frac{ch}{PF \cdot D^2 \cdot De}\right] + 401.5 \cdot \left[\frac{I}{PF \cdot D^2 \cdot De}\right] \\ & - 6.99 \times 10^{-5} \cdot \left[\frac{\theta \cdot D}{De}\right] + 5.95 \times 10^{-5} \cdot \left[\frac{\delta \cdot D}{De}\right] \end{aligned} \tag{21}$$

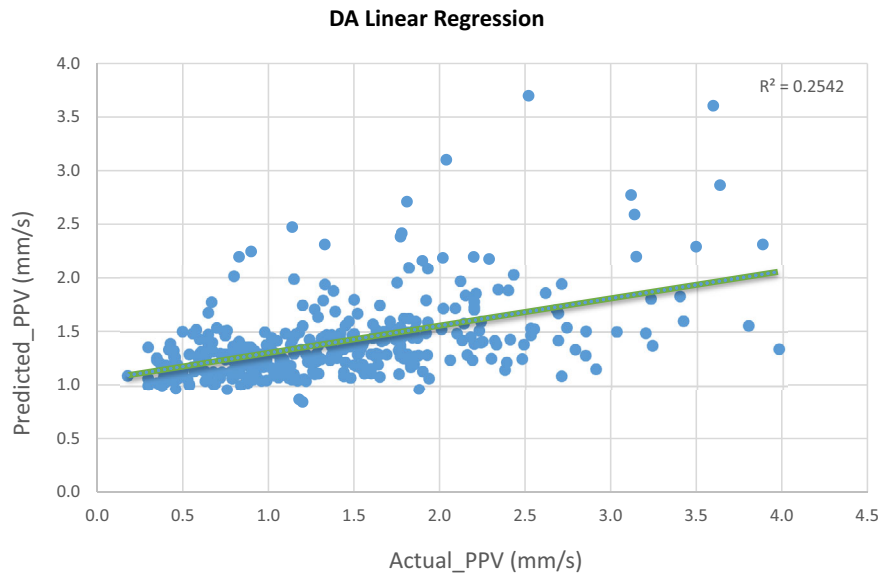


Figure 1. Actual PPV versus predicted PPV by DA using linear regression analysis.

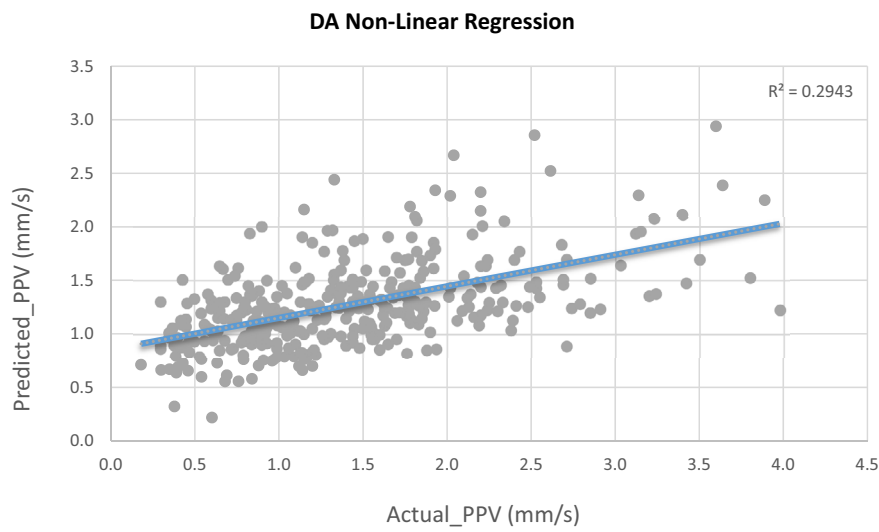


Figure 2. Actual PPV versus predicted PPV by DA using nonlinear regression analysis.

Table 11. Errors between predicted and actual PPV values when a single set of site constants is used

Error index	Linear	Nonlinear
R^2	25.42%	29.15%
MAE	0.4953	0.4802
RMSE	0.6345	0.6321

the linear DA regression. The errors associated with the linear and nonlinear predictions are listed in Table 12.

Conventional Predictors

The blast monitoring data from the gold mine were used to determine site constants for the four

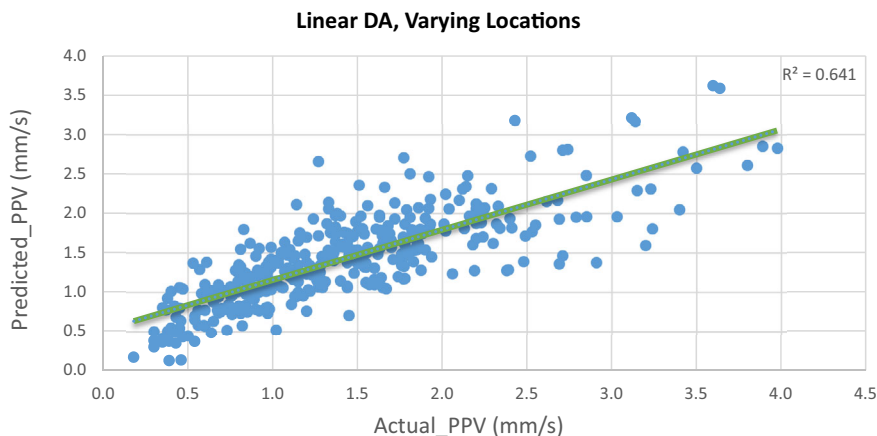


Figure 3. Actual PPV versus predicted PPV by DA using linear regression considering location characteristics.

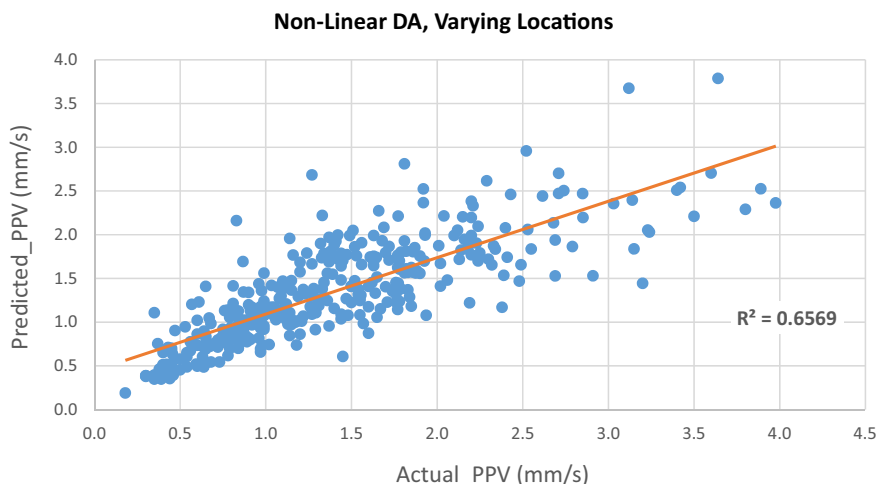


Figure 4. Actual PPV versus predicted PPV by DA using nonlinear regression considering location characteristics.

Table 12. Comparison of actual with predicted PPV values considering location characteristics

Error index	Linear regression	Nonlinear regression
R^2	63.99%	65.69%
MAE	0.3296	0.3111
RMSE	0.4428	0.4362

conventional predictor models depicted in Table 6. The site constants of these four conventional predictor equations are shown in Table 13.

Figures 5, 6, 7, 8 illustrate the relationships between predicted PPV values and actual PPV values for each of the equations in Table 13. Table 14 shows the errors in terms of R^2 , MAE and RMSE between the predicted and actual PPV levels for the four conventional equations. It can be seen that the R^2 ranged from 0.1116 to 0.1611, and the Ambraseys–Hendron predictor equation showed the highest R^2 and lowest errors among all the four conventional predictor equations.

Table 13. Site constants for the conventional predictor equations

Conventional predictor	Site constant K	Site constant B
$PPV = K \left(\frac{D}{\sqrt{MIC}} \right)^{-B}$	$e^{5.4146} = 224.663$	- 1.1304
$PPV = K \left(\sqrt{\frac{MIC}{D^3}} \right)^B$	$e^{0.5561} = 1.744$	1.0136
$PPV = K \left(\frac{D}{MIC^{\frac{1}{3}}} \right)^{-B}$	$e^{8.9243} = 7512.323$	- 1.6761
$PPV = K \left(\frac{MIC}{D^3} \right)^B$	$e^{0.5561} = 1.744$	0.5068

Conventional Predictors—Segregation of Site Constants for Comparable Conditions

Because, among the four conventional predictor equations, the Ambraseys–Hendron predictor equation got the highest R^2 and with least MAPE and RMSE for the predicted PPV compared to actual PPV, it was employed further using segregated data to compare constant characteristics relating to

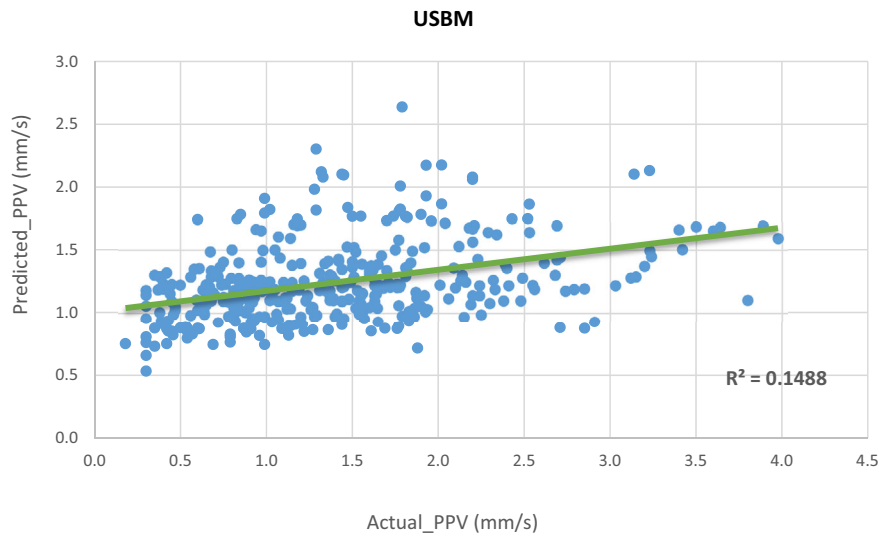


Figure 5. Actual PPV versus predicted PPV by the USBM equation.

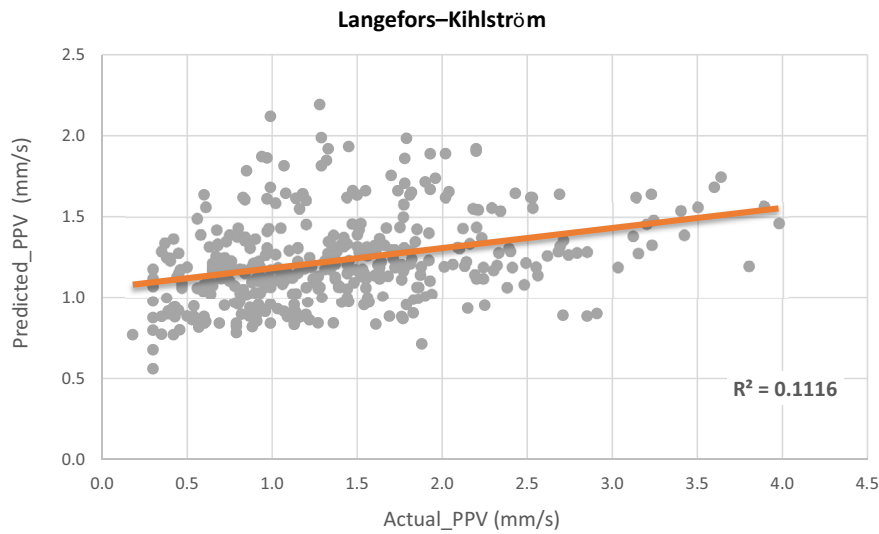


Figure 6. Actual PPV versus predicted PPV by the Langefors-Kihlström equation.

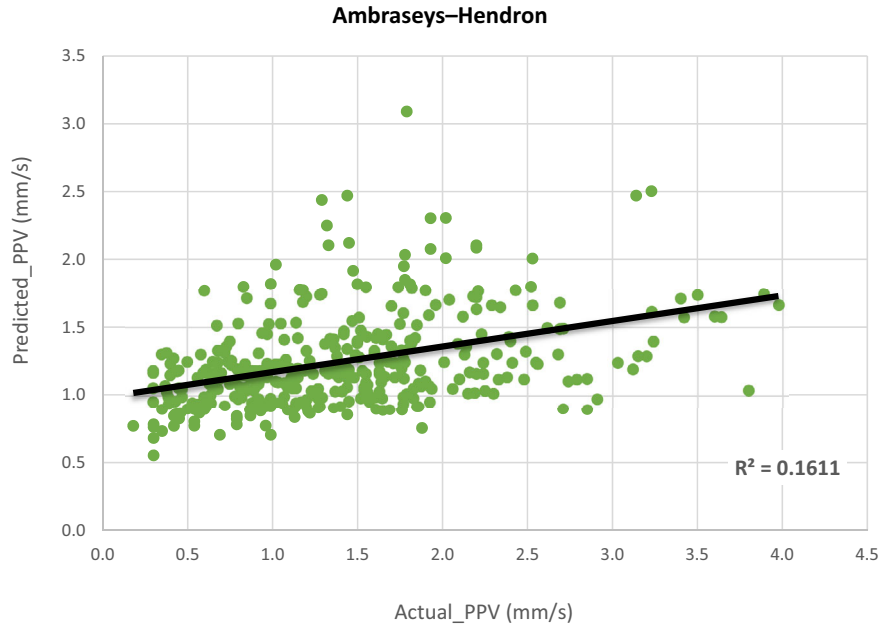


Figure 7. Actual PPV versus predicted PPV by the Ambraseys-Hendron equation.

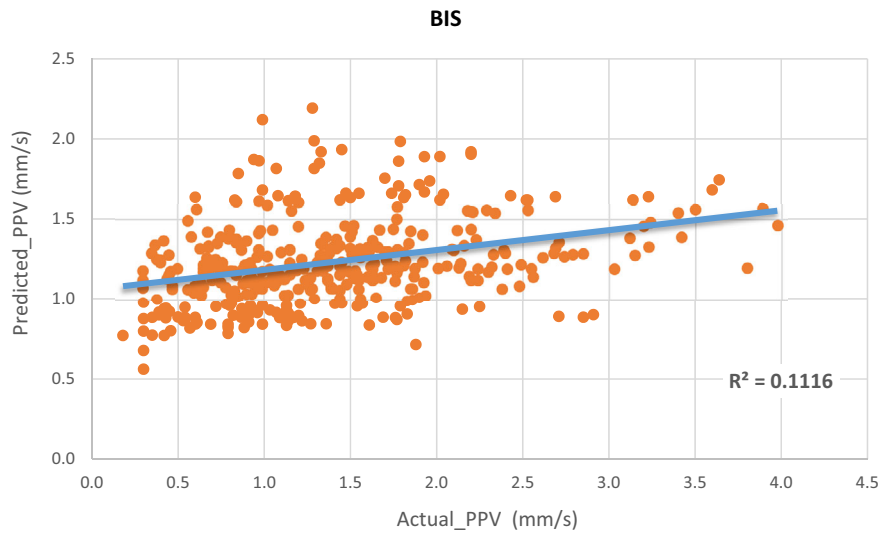


Figure 8. Actual PPV versus predicted PPV by the BIS equation.

distance between the blast location and the monitoring site. Figure 9 shows a plot of actual PPV versus predicted PPV by the Ambraseys-Hendron equation considering location characteristics. The R^2 was 0.4098, MAE 0.4145 and RMSE 0.5762 (Table 15).

Validation of Effectiveness of DA vs Conventional Models

A new set of ten data points was used to compare the effectiveness of the segregated nonlinear DA equation and the Ambraseys-Hendron equation (Tables 16, 17, 18, 19).

Table 14. Comparison of actual PPV and predicted PPV using the conventional predictor equations

Error index	USBM	Langefors-Kihlstrm	Ambraseys-Hendron	BIS
R^2	14.88%	11.16%	16.11%	11.16%
MAE	0.53	0.55	0.53	0.55
RMSE	0.71	0.72	0.70	0.72

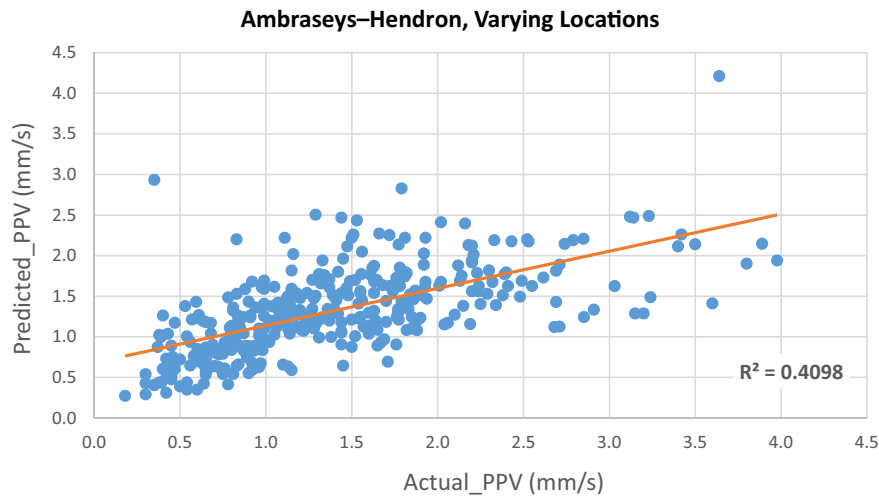


Figure 9. Actual PPV versus predicted PPV using the Ambraseys-Hendron equation considering location characteristics.

Table 15. Comparison between the predicted and actual PPV's for the Ambraseys-Hendron equation when site constants based on location characteristics are considered

Error index	Ambraseys-Hendron
R^2	40.98%
MAE	0.4145
RMSE	0.5762

Figure 10 depicts the comparison of the nonlinear DA model and the Ambraseys-Hendron model. Table 20 shows the errors in terms of R^2 , MAE and RMSE between the predicted and actual PPV levels for the nonlinear DA equation and the Ambraseys-Hendron equation. From Figure 10, it can be said that nonlinear DA model yielded higher R^2 and less errors.

DISCUSSION

Effectiveness of Conventional Predictors

The test conducted at the gold mine supports the claim that no single conventional predictor equation is accurate to predict PPV. If conventional predictor equations are used at a mine location, all of them need to be analyzed and compared to one another to determine the most appropriate model.

On examining the recorded data at the mine, it was found that, of the four conventional predictor equations analyzed, the Ambraseys-Hendron equation was the most accurate. It had a 16.11% R^2 whereas the USBM equation had a lower R^2 of 14.88% (Table 14). This means that, compared to the USBM equation, the Ambraseys-Hendron equation has a slightly higher chance of predicted PPV values falling on the regression line. The Ambraseys-Hendron equation also had slightly lower RMSE and MAE compared to the USBM equation, meaning that the average errors between the actual

Table 16. Set of results used to compare the accuracy of the segregated DA model against the Ambraseys–Hendron model

Monitor site	Mine section	D	θ	δ	PF	ch	I	De	R	MIC	PPV
A	BRT	599	56	56	0.46	960	191	1.70	2,501	39.2	1.38
B	LLB	747	38	56	2.05	1,200	234	4.70	700	70.0	0.84
B	LLB	747	24	45	1.12	993	219	5.59	1,087	73.3	1.08
C	BRT	599	32	30	1.20	876	129	4.55	1,000	42.0	1.44
C	BRT	599	91	103	0.98	2,391	276	6.30	2,713	62.8	0.93
B	LLB	747	39	81	2.29	2,437	409	8.49	1,242	129.3	1.28
C	LLB	712	24	41	4.05	760	160	4.45	227	52.6	0.97
C	LLB	712	28	41	1.25	810	70	4.17	674	47.4	0.37
D	LLB	747	24	41	1.09	950	185	5.60	1,046	70.4	0.97
C	BRT	576	63	113	0.83	2,800	310	6.80	3,646	82.3	2.20

Table 17. DA by using the log of modified dimensionless variables in Eq. 20

$\ln(\text{PPV})$	$\ln\left(\frac{\text{MIC}}{\text{PF} \cdot D^2 \cdot \text{De}}\right)$	$\ln\left(\frac{R}{\text{PF} \cdot D^2 \cdot \text{De}}\right)$	$\ln\left(\frac{\text{ch}}{\text{PF} \cdot D^2 \cdot \text{De}}\right)$	$\ln\left(\frac{I}{\text{PF} \cdot D^2 \cdot \text{De}}\right)$	$\ln\left(\frac{\theta \cdot D}{\text{De}}\right)$	$\ln\left(\frac{\delta \cdot D}{\text{De}}\right)$
0.32	- 8.88	- 4.72	- 5.68	- 7.29	9.89	9.89
- 0.17	- 11.25	- 8.95	- 8.41	- 10.04	8.71	9.09
0.08	- 10.77	- 8.08	- 8.17	- 9.68	8.07	8.70
0.36	- 10.75	- 7.58	- 7.71	- 9.63	8.35	8.28
- 0.07	- 10.92	- 7.45	- 7.53	- 9.05	9.08	9.08
0.25	- 11.34	- 9.08	- 8.40	- 10.19	8.14	8.87
- 0.03	- 12.07	- 10.60	- 9.39	- 10.95	8.25	8.79
- 0.99	- 10.93	- 8.27	- 8.09	- 10.54	8.47	8.85
- 0.03	- 10.79	- 8.09	- 8.18	- 9.82	8.07	8.61
0.79	- 10.03	- 6.24	- 6.51	- 8.71	8.58	9.17

Table 18. DA by using site constants relating to relevant field in Eq. 20

Monitor site		k	x_2	x_3	x_4	x_5	x_6	x_7	Predicted PPV
C	BRT	6.15	- 0.20	- 0.22	0.95	0.03	- 0.20	- 0.08	1.81
B	LLB	- 2.54	- 0.41	0.26	0.15	- 0.01	- 0.49	0.63	1.13
B	LLB	- 2.54	- 0.41	0.26	0.15	- 0.01	- 0.49	0.63	1.27
C	BRT	6.15	- 0.20	- 0.22	0.95	0.03	- 0.20	- 0.08	1.04
C	BRT	6.15	- 0.20	- 0.22	0.95	0.03	- 0.20	- 0.08	1.02
B	LLB	- 2.54	- 0.41	0.26	0.15	- 0.01	- 0.49	0.63	1.30
C	LLB	3.72	0.24	- 0.55	0.94	0.09	- 0.84	1.11	0.66
C	LLB	3.72	0.24	- 0.55	0.94	0.09	- 0.84	1.11	0.75
D	LLB	- 11.13	- 0.72	0.09	0.38	- 0.04	- 0.34	1.10	0.93
C	BRT	6.15	- 0.20	- 0.22	0.95	0.03	- 0.20	- 0.08	1.91

PPV and the predicted PPV using the Ambraseys–Hendron equation were lower than those using the USBM equation.

Effectiveness of DA Predictors

It was theorized that, to increase the accuracy of predictions, a variety of variables that influence predictions need to be incorporated into the prediction model. Dropping a pebble into a pond creates waves that can be measured accurately. The

Table 19. Relevant variable results required to predict PPV using the Ambraseys–Hendron equation

Monitor site	Mine section	$\frac{D}{MIC^{\frac{1}{3}}}$	K	B	$PPV = K \left(\frac{D}{MIC^{\frac{1}{3}}} \right)^B$
C	BRT	176.332	134,014	- 2.283	1.00
B	LLB	181.254	66.933	- 0.764	1.26
B	LLB	178.492	66.933	- 0.764	1.27
C	BRT	172.323	134,014	- 2.283	1.05
C	BRT	191.508	134,014	- 2.283	0.83
B	LLB	147.725	66.933	- 0.764	1.47
C	LLB	190.028	75,109	- 2.151	0.94
C	LLB	196.738	75,109	- 2.151	0.87
D	LLB	180.91	676.25	- 1.194	1.36
C	BRT	132.421	134,014	- 2.283	1.92

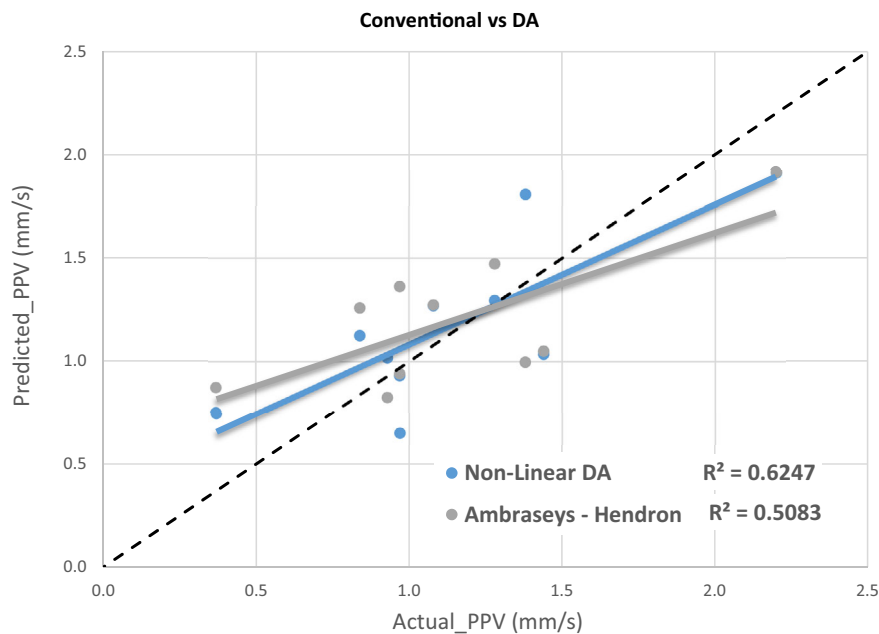


Figure 10. Plots to compare the nonlinear DA model and the Ambraseys–Hendron model. Dotted line represents the perfect relationship between actual and predicted values.

Table 20. Comparison of the nonlinear DA and the Ambraseys–Hendron models

Error index	Nonlinear DA	Ambraseys–Hendron
R^2	62.47%	50.83%
MAE	0.24	0.29
RMSE	0.28	0.32

reason for this is that enough information to fully describe the phenomenon is known. Water as a

medium is uniform and the characteristics of the force impacting this medium can be calculated. Blasting can be compared to this analogy, where the medium is the surrounding rock, which is highly variable making vibration waves challenging to measure. The location of the blast is never in the same spot, meaning that relationships between variables are problematic to analyze. However, including more factors that describe wave propagation will increase the accuracy of future predictions. For this reason, a DA approach was used to relate the influencing factors to increase the accuracy of

the predictions made at the mine. The equation developed also needed to be usable, whereby the variables chosen to construct the equation are based on variables that the mine already measured and recorded. This means that if a model was to replace the current system, no additional measurements that were not already recorded should be used.

In this study, all the variables were used except for the diameters and lengths of blast holes. The diameters of the blast holes are the same for all blasts, which effectively means that it will not affect the results, and so adding this variable serves no real purpose. There is no consistency to the lengths of the blast holes, whereby most of them have differing lengths for each blast. If the relationship on how a set of blast hole lengths affects PPV were to be analyzed, all holes for a single blast must be the same. Another approach to analyzing this relationship is to use the longest blast hole for a given blast, because the longer the hole, the more explosive will be set off when the hole is detonated. Instead, the *MIC* can be employed. It can be suggested that the greater the hole lengths, the higher the *MIC*, because there will be more explosives in a given hole. Therefore, the *MIC* makes the effects of altering the hole lengths redundant.

To inspect the dimensionless groups, both linear and nonlinear multiple regression analyses were used. When comparing the predicted PPV values against the actual PPV values, it was found that the nonlinear regression model proved to be dominant. It had a stronger relationship with an R^2 of 29.15% compared to linear model's R^2 of 25.42% (Table 11). Additionally, the nonlinear regression model had a lower RMSE of 0.632 compared to linear regression model's 0.635. Moreover, the MAE of nonlinear regression model was lower than the linear regression model's 0.480. For the data collected, it was found that some predicted PPV values of the linear regression model were negative, which is theoretically impossible. To negate this issue, an absolute function on the predicted PPV was taken.

Segregating Site Constants Based on Location Characteristics

The distance used in the analysis using both the conventional predictors and the DA models is the vertical depth of the blast. If the monitoring site was directly above the blast location, then this distance would be an accurate representation of the distance

traveled by the blast vibrations. The straight-line diagonal distance between the blast location and the monitoring site (Fig. 11) would be a more accurate representation of the distance. This diagonal distance is not recorded, however, which would mean that the horizontal distance between the monitoring site and the blast location is required to work out this diagonal distance. The gold mine records the section of the mine where the blast is undertaken, as well as the monitoring site used to measure the PPV. However, not all blasts for a section of the mine are recorded at the same monitoring station. Within each mine section, the vertical depth is recorded as depicted in Figure 11. Section A for example, can use any of the monitoring stations, where it is clear that the distance between section A and M2 is less than the distance between A and M4. The issue is that the results are being analyzed on the assumption that differences in horizontal distance between mine sections and monitoring stations do not affect the distance traveled by the blast waves. However, this is an important factor that needs to be addressed.

To overcome the above problems, the results were grouped into their respective mine sections and then again for each monitoring station. This is allowed for the vertical depth to provide a more accurate distance measure, as it can essentially negate the effect of the horizontal distance. The vertical distances would then become beneficial for comparing how the depth within each mine section would affect the PPV at the same monitoring stations. Analysis of the blast monitoring data showed that there were 15 combinations between the various sections of the mines and the monitoring sites. A set of site constants was generated for each of these combinations for the most accurate DA model, which was by nonlinear regression, and the most accurate conventional predictor, which was the Ambraseys–Hendron equation. From Figure 4, which presents the plots of the predicted PPV versus actual PPV, it was found that, by segregating the data into comparable conditions, the MAE was reduced from 0.480 to 0.311 and the RMSE was reduced from 0.632 to 0.436. In addition, the R^2 increased from 29.15% to 65.69%. For the Ambraseys–Hendron equation, similar outcomes were achieved when the adjusted distance traveled by the vibrations was considered (Fig. 9), improved accuracy scores of MAE = 0.415, RMSE = 0.576 and R^2 = 40.98% (Table 15).

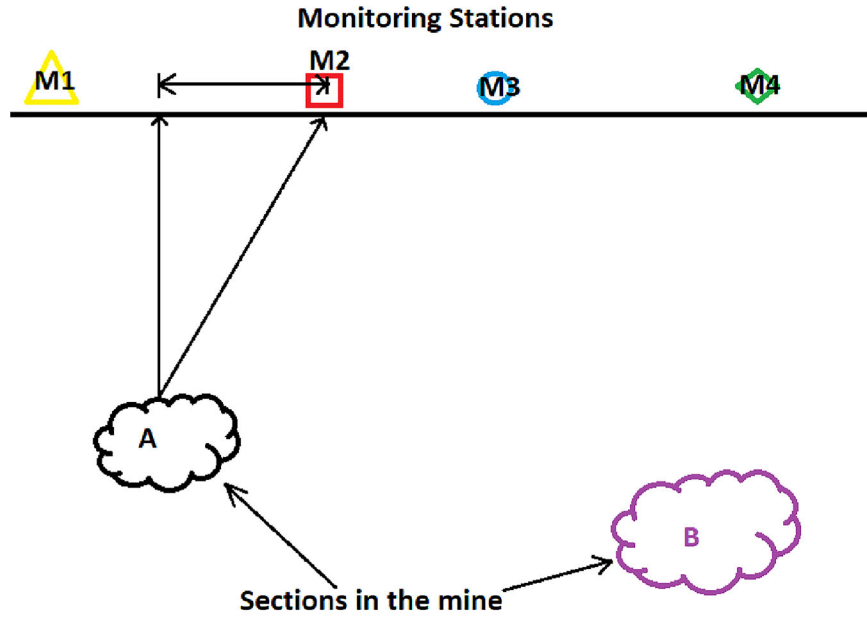


Figure 11. Representation of the monitoring site locations in respect to the mine sections.

Comparison between DA and Conventional Predictors

By analyzing the accuracy scores, it was determined that the DA approach was more accurate than the conventional predictors, but the latter were easier to use. The most effective conventional predictor had a R^2 of 16.11% whereas the nonlinear DA equation had a R^2 of 29.15%. The RMSE and MAE for the nonlinear DA equation were also lower than the most effective conventional predictor. These results support the hypothesis that more variables that affect PPV are required to improve the accuracy of the predictions made. While it is important to incorporate a range of parameters, not all parameters necessarily improve the quality of the DA model. Many researchers (Dehghani & Ataee-pour, 2011; Khandelwal & Saadat, 2015) came up with the same conclusions. Only using quantity of explosives and distance does not incorporate enough variables to model PPV, whereas the only benefit to using the conventional predictors is that they can be used as a quick measure to predict PPV roughly.

To further demonstrate the concept of including more variables that affect PPV, the vertical distance measure was modified to incorporate variations in horizontal distance. This was done for the most effective DA model as well as the most effective

conventional predictor. A new set of data was retrieved to analyze the effectiveness of each of these two models. Comparing the regression lines to the perfect regression line in figure, it is evident that the DA model was more effective. It is clear that, compared to the Ambraseys–Hendron equation with R^2 of 50.87%, the nonlinear DA equation with R^2 of 62.47% resembles more closely the perfect regression line. It is evident further that the average errors of regression lines were higher for the Ambraseys–Hendron equation than for the nonlinear DA equation.

The model for predicting PPV in the gold mine depends, therefore, on what the users of the model wish to achieve. If a quick and rough estimate is required, the Ambraseys–Hendron equation with one set of site constants can be used, thus:

$$PPV = 7512.323 \left(\frac{D}{MIC^{\frac{1}{3}}} \right)^{-1.6761}$$

Using this equation is immensely simple once a computing program has been set up to calculate PPV automatically. This model can be the suggested method for many mining operations located near residential areas, because to be able to predict PPV effectively can improve business performance. For example, increasing the PPV prediction capability

reduces the need to incorporate unnecessarily high safety factors.

CONCLUSIONS

Dimensional analysis (DA) and conventional predictors were used to study the blast vibration levels at one of the underground gold mines in Australia. For the study, a DA approach was employed to develop an equation that can increase PPV prediction accuracy at the mine site. The current model used at the mine is the United States Bureau of Mines (USBM) equation, which is one of the many conventional predictors that have been developed in the past. Conventional predictors incorporate the maximum explosive charge at any given time and the distance from the monitoring point to the blast location. However, DA includes other parameters that provide additional effect on wave propagation.

Most of the conventional predictors are based on only two to three parameters (i.e., explosive charge per delay, distance between blast face to monitoring point, attenuation factor), whereas it is a well-known fact that blast vibrations are influenced by various blast designs, explosives and rock parameters. Thus, here, a greater number of blast design parameters were taken into consideration with the help of DA to assess and evaluate blast vibrations due to underground mining and a new, simple and easy-to-use blast vibrations equation was proposed to evaluate and predict underground blast vibrations in an effective and efficient manner.

It was found that the DA equation obtained by nonlinear multiple regression had the highest accuracy scores. The data also showed that of the four conventional predictors, the Ambraseys–Hendron equation was the most effective at the gold mine. These two models were compared directly to one another to validate the effectiveness of the DA model. Before the models were compared, the vertical depth used as the distance for the two equations was modified by grouping data with similar horizontal distances between blasts and monitoring sites. This process reduced the effect of the horizontal variance, which proved to greatly increase the accuracy of prediction. To validate the results, ten new sets of blast data were obtained and used in where equations predict PPV. The R^2 of the nonlinear DA equation was found to be 0.62 as opposed to 0.51 for the Ambraseys–Hendron equation (Ta-

ble 20), and the RMSE for the DA model was 0.28 compared to 0.32 for the Ambraseys–Hendron equation.

By analyzing all the data, it was suggested that the DA model is used when a higher degree of accuracy between predicted and actual PPV is required. The advantage of a DA model is that there are little restrictions on the selection of important variables, and its predictive capability increases when more of these important variables are added to the model. The only main drawback of the DA approach compared to the conventional predictors is that it can take longer to set up. However, adding irrelevant parameters that show no relationship can taint the results. In future, a greater number of appropriate blast design, explosive and rock parameters can be taken into consideration to develop a more generalized blast vibration equation.

REFERENCES

- Afeni, T. B., & Osasan, S. K. (2009). Assessment of noise and ground vibration induced during blasting operations in an open pit mine—A case study on Ewekoro limestone quarry, Nigeria. *Mining Science and Technology (china)*, 19(4), 420–424.
- Alhama, F., & Madrid, C. N. (2007). Discriminated dimensional analysis versus classical dimensional analysis, Applications to heat transfer and fluid dynamics. *CJChE*, 15(5), 626–631.
- Alvarez-Vigil, A. E., Gonzales-Nicieza, C., Lopez Gayarre, F., & Alvarez-Fernandez, M. I. (2012). Predicting blasting propagation velocity and vibration frequency using artificial neural network. *International Journal of Rock Mechanics and Mining Sciences*, 55, 108–116.
- Armaghani, D. J., Momeni, E., Abad, S. V. A. N. K., et al. (2015). Feasibility of ANFIS model for prediction of ground vibrations resulting from quarry blasting. *Environment and Earth Science*, 74, 2845–2860.
- Bakhshandeh Amnieh, H., Siamaki, A., & Soltani, S. (2012). Design of blasting pattern in proportion to the peak particle velocity (PPV): Artificial neural networks approach. *Safety Science*, 50(9), 1913–1916.
- Bakhtavar, E., Abdollahisharif, J., & Ahmadi, M. (2017b). Reduction of the undesirable bench-blasting consequences with emphasis on ground vibration using a developed multi-objective stochastic programming. *International Journal of Mining, Reclamation and Environment*, 31(5), 333–345.
- Bakhtavar, E., Khoshrou, H., & Badroddin, M. (2015). Using dimensional-regression analysis to predict the mean particle size of fragmentation by blasting at the Sungun copper mine. *Arabian Journal of Geosciences*, 8, 2111–2120.
- Bakhtavar, E., Nourizadeh, H., & Sahebi, A. A. (2017a). Toward predicting blast-induced flyrock: A hybrid dimensional analysis fuzzy inference system. *International Journal of Environmental Science and Technology*, 14, 717–728.
- Bakhtavar, E., & Yousefi, S. (2019). Analysis of ground vibration risk on mine infrastructures: Integrating fuzzy slack-based measure model and failure effects analysis. *International*

- Journal of Environmental Science and Technology*, 16, 6065–6076.
- Bayat, P., Monjezi, M., Mehrdaneh, A., et al. (2021). Blasting pattern optimization using gene expression programming and grasshopper optimization algorithm to minimise blast-induced ground vibrations. *Engineering with Computers*. <http://doi.org/10.1007/s00366-021-01336-4>.
- Bui, X. N., Nguyen, H., Tran, Q. H., et al. (2021). Predicting ground vibrations due to mine blasting using a novel artificial neural network-based cuckoo search optimization. *Natural Resources Research*, 30, 2663–2685.
- Bureau of Indian Standard. (1973). Criteria for safety and design of structures subjected to underground blast.
- Chen, S., Zhang, Z., & Wu, J. (2015). Human comfort evaluation criteria for blast planning. *Environmental Earth Sciences*, 74(4), 2919–2923.
- Cheng, C. L., & Garg, G. (2014). Coefficient of determination for multiple measurement error models. *Journal of Multivariate Analysis*, 126, 137–152.
- Cheng, K. M., & Chau, K. T. (2015). *Attenuation of blasting induced peak particle velocity: Constructing a new empirical formula*. Crc Press-Taylor & Francis Group.
- Dehghani, H., & Ataee-pour, M. (2011). Development of a model to predict peak particle velocity in a blasting operation. *International Journal of Rock Mechanics and Mining Sciences*, 48(1), 51–58.
- Ding, Z., Nguyen, H., Bui, X. N., et al. (2020). Computational intelligence model for estimating intensity of blast-induced ground vibration in a mine based on imperialist competitive and extreme gradient boosting algorithms. *Natural Resources Research*, 29, 751–769.
- Duvall, W. I., Fogelson, D. E., & USBM. (1962). *Review of criteria for estimating damage to residences from blasting vibrations*. Retrieved from <http://www.osmre.gov/resources/blasting/docs/USBM/R15968EstimatingDamagesResidences.pdf>.
- Fang, Q., Nguyen, H., Bui, X. N., et al. (2020). Prediction of blast-induced ground vibration in open-pit mines using a new technique based on imperialist competitive algorithm and M5Rules. *Natural Resources Research*, 29, 791–806.
- Fattahi, H., & Hasanipanah, M. (2021). Prediction of blast-induced ground vibration in a mine using relevance vector regression optimized by metaheuristic algorithms. *Natural Resources Research*, 30, 1849–1863.
- Fisne, A., Kuzu, C., & Hudaverdi, T. (2011). Prediction of environmental impacts of quarry blasting operation using fuzzy logic. *Environmental Monitoring and Assessment*, 174(1–4), 461–470.
- He, Z., Armaghani, D. J., Masoumnezhad, M., et al. (2021). A combination of expert-based system and advanced decision-tree algorithms to predict air-overpressure resulting from quarry blasting. *Natural Resources Research*, 30, 1889–1903. <https://doi.org/10.1007/s11053-020-09773-6>.
- Hendron, A., & Ambraseys, N. (1968). *Dynamic behaviour of rock masses (Zienkiewicz OC ed)*. Wiley.
- Khandelwal, M. (2010). Evaluation and prediction of blast induced ground vibration using support vector machine. *International Journal of Rock Mechanics & Mining Sciences*, 47(3), 509–516.
- Khandelwal, M. (2011). Blast-induced ground vibration prediction using support vector machine. *Engineering with Computers*, 27(3), 193–200.
- Khandelwal, M. (2012). Application of an expert system for the assessment of blast vibration. *Geotechnical and Geological Engineering*, 30(1), 205–217.
- Khandelwal, M., Armaghani, D. J., Faradonbeh, R. S., et al. (2017). Classification and regression tree technique in estimating peak particle velocity caused by blasting. *Engineering with Computers*, 33(1), 45–53.
- Khandelwal, M., Kankar, P. K., & Harsha, S. P. (2010). Evaluation and prediction of blast induced ground vibration using support vector machine. *Mining Science and Technology (china)*, 20(1), 64–70.
- Khandelwal, M., Kumar, D. L., & Yellishetty, M. (2011). Application of soft computing to predict blast-induced ground vibration. *Engineering with Computers*, 27(2), 117–125.
- Khandelwal, M., & Saadat, M. (2015). A dimensional analysis approach to study blast-induced ground vibration. *Rock Mechanics and Rock Engineering*, 48(2), 727–735.
- Khandelwal, M., & Singh, T. N. (2006). Prediction of blast induced ground vibrations and frequency in opencast mine: A neural network approach. *Journal of Sound and Vibration*, 289(4–5), 711–725.
- Khandelwal, M., & Singh, T. N. (2007). Evaluation of blast-induced ground vibration predictors. *Soil Dynamics and Earthquake Engineering*, 27(2), 116–125.
- Khandelwal, M., & Singh, T. N. (2009). Prediction of blast-induced ground vibration using artificial neural network. *International Journal of Rock Mechanics and Mining Sciences*, 46(7), 1214–1222.
- Khandelwal, M., & Singh, T. N. (2013). Application of an expert system to predict maximum explosive charge used per delay in surface mining. *Rock Mechanics and Rock Engineering*, 46(6), 1551–1558.
- Langefors, U., & Kihlström, B. (1963). *The modern technique of rock blasting* (Vol. 1). Wiley.
- Mohamadnejad, M., Gholami, R., & Ataee, M. (2012). Comparison of intelligence science techniques and empirical methods for prediction of blasting vibrations. *Tunnelling and Underground Space Technology*, 28, 238–244.
- Mohammad, M. T. (2009). Artificial neural network for prediction and control of blasting vibration in Assiut (Egypt) limestone quarry. *International Journal of Rock Mechanics and Mining Sciences*, 46(2), 426–431.
- Monjezi, M., Hasanipanah, M., & Khandelwal, M. (2013). Evaluation and prediction of blast-induced ground vibration at Shur River Dam, Iran, by artificial neural network. *Neural Computing and Applications*, 22(7/8), 1637–1643.
- Monjezi, M., Singh, T. N., Khandelwal, M., Sinha, S., Singh, V., & Hosseini, I. (2006). Prediction and analysis of blast parameters using artificial neural network. *Noise & Vibration Worldwide*, 37(5), 8–16.
- Qiu, Y., Zhou, J., Khandelwal, M., Yang, H., Yang, P., & Li, C. (2021). Performance evaluation of hybrid WOA-XGBoost, GWO-XGBoost and BO-XGBoost models to predict blast-induced ground vibration. *Engineering with Computers*. <http://doi.org/10.1007/s00366-021-01393-9>.
- Reddy, G. M., & Reddy, V. D. (2014). Theoretical investigations on dimensional analysis of ball bearing parameters by using buckingham pi-theorem. *Procedia Engineering*, 97, 1305–1311.
- Rezaeineshat, A., Monjezi, M., Mehrdaneh, A., et al. (2020). Optimization of blasting design in open pit limestone mines with the aim of reducing ground vibration using robust techniques. *Geomechanics and Geophysics for Geo-Energy and Geo-Resources*, 6, 1–14.
- Saadat, M., Hasanzade, A., & Khandelwal, M. (2015). Differential evolution algorithm for predicting blast induced ground vibrations. *International Journal of Rock Mechanics and Mining Sciences*, 77, 97–104.
- Saadat, M., Khandelwal, M., & Monjezi, M. (2014). An ANN-based approach to predict blast-induced ground vibration of Gol-E-Gohar iron ore mine, Iran. *Journal of Rock Mechanics and Geotechnical Engineering*, 6(1), 67–76.
- Sanchidrián, J. A., & Ouchterlony, F. A. (2017). Distribution-free description of fragmentation by blasting based on dimensional analysis. *Rock Mechanics and Rock Engineering*, 50, 781–806.

- Sharp, J. J., Deb, A., & Deb, M. K. (1992). Applications of matrix manipulation in dimensional analysis involving large numbers of variables. *Marine Structures*, 5(4), 333–348.
- Simangunsong, G. M., & Wahyudi, S. (2015). Effect of bedding plane on prediction blast-induced ground vibration in open pit coal mines. *International Journal of Rock Mechanics and Mining Sciences*, 79, 1–8.
- Zhang, X., Nguyen, H., Bui, X. N., Tran, Q. H., Nguyen, D. A., Bui, D. T., & Moayedi, H. (2020). Novel soft computing model for predicting blast-induced ground vibration in open-pit mines based on particle swarm optimization and XGBoost. *Natural Resources Research*, 29(2), 711–721.